Journal of
Nanoscience and Nanotechnology
Vol. 7, 1–5, 2007

Organometallic Radical-Adducts of Fullerenes C_{60}, C_{70}, and Single-Walled Carbon Nanotubes Derived from (Cyclopentadienyl)molybdenumtricarbonyl Dimer

Rashid G. Gasanov[1], Anatolii S. Lobach[2,*], Viatcheslav I. Sokolov[1], Aleksei P. Demenjev[3], Konstantin I. Maslakov[3], and Elena D. Obraztsova[4]

[1] *Institute of Organoelement Compounds, Russian Academy of Sciences, 28 Vavilov Street, 119991 Moscow, Russia*
[2] *Institute of Problems of Chemical Physics, Russian Academy of Sciences, 142432 Chernogolovka, Moscow Region, Russia*
[3] *Russian Research Centre "Kurchatov Institute", Kurchatov sq. 1, 123182 Moscow, Russia*
[4] *Natural Sciences Center of General Physics Institute Russian Academy of Sciences, 38 Vavilov Street, 119899 Moscow, Russia*

Interaction of the metal-centered free radicals $[CpMo(CO)_3]^\bullet$ generated photochemically from the corresponding dimer $[CpMo(CO)_3]_2$ with fullerenes C_{60}, C_{70}, or single-walled carbon nanotubes in toluene results in the radical-adducts investigated by using TGA, ESR, Raman and X-ray Photoelectron spectroscopy. Comparison was made with the chromium analogues previously studied.

Keywords: (Cyclopentadienyl)molybdenumtricarbonyl Dimer, Molybdenum-Centered Free Radical, Fullerenes C_{60}, C_{70}, Single-Walled Carbon Nanotubes, Radical-Adducts, ESR Spectroscopy, Raman, X-ray Photoelectron Spectroscopy.

RESEARCH ARTICLE

1. INTRODUCTION

Fullerenes are known to readily add free radicals to give the adducts stable in solution under inert atmosphere.[1–3] Addition of odd number of these species affords paramagnetic radical-adducts which can be successfully investigated by ESR spectroscopy.

Our research group had previously introduced phosphoryl radicals derived photolytically from the mercuric compounds (Scheme 1) as a convenient tool to characterize fullerene derivatives owing to the additional information obtained from the hyperfine splitting (*hfs*) constant *a* due to the magnetic nucleus ^{31}P in the key position of the phosphoryl radical.[4–6]

$$[(AlkO)_2P(O)]_2Hg \xrightarrow{h\nu} [(AlkO)_2P(O)]^\bullet$$

Scheme 1

The first addition of the *metal*-centered free radical to fullerene C_{60} had been achieved by using photolysis of the precursor containing a platinum-mercury bond.[7]

Recently we have reported[8] the study of the addition to fullerenes of the chromium-centered free radicals generated at room temperature in toluene by the easy homolytical dissociation of the metal–metal bond in cyclopentadienylchromiumtricarbonyl dimers (Scheme 2).

$$[CpM(CO)3]_2 + C_n \rightarrow \{CpM(CO)_2(\eta^2 - C_n)\}^\bullet,$$
$$Cp = C_5H_5, C_5Me_5; M = Cr; n = 60, 70$$

Scheme 2

There is an obvious structural similarity between fullerenes and carbon nanotubes based on the strained double bonds between neighboring hexagons incorporated. However, the resemblance in reactivity versus free radicals is limited by the competition of oxygen atoms if carbon nanotubes have been oxidized.

More recently we have used the above-mentioned chromium reagent in the treatment of the oxidized single-walled carbon nanotubes (SWNT) and observed the ESR signal which according to its g-factor corresponded to bonding the chromium atom with oxygen rather than carbon that was confirmed by Raman spectra as well.[9]

2. EXPERIMENTAL DETAILS

2.1. Synthesis

Fullerenes C_{60} (99.9% pure) and C_{70} (99.5% pure) were purchased from the Institute of Organometallic Chemistry (Nizhny-Novgorod, Russia), cyclopentadienylmolybdenumtricarbonyl dimer from Strem Chemicals. The raw materials of high pressure carbon monoxide

*Author to whom correspondence should be addressed.

decomposition (HiPco) SWNT were purchased from Carbon Nanotechnologies, Inc. and purified according to existing purification protocols modified by us.[10–11] The Fe metal and oxygen content after purification was measured by X-ray photoelectron spectroscopy and was determined to be approximately 0.4 and 4 at.%, respectively.

Glass cylinder ampoules were charged with $4.9 \cdot 10^{-4}$g ($1.0 \cdot 10^{-3}$ mM) of solid $[CpMo(CO)_3]_2$, evacuated and filled with argon several times then solution of fullerene (C_{60} or C_{70}) was added and the ampoule was subjected to several "freeze-thaw" cycles and finally sealed under argon. Irradiation was carried out using 100 W lamp outside the ESR instrument during several hours. SWNT sample as a suspension in toluene was sonicated then $[CpMo(CO)_3]_2$ was added and the ampoule was treated as in the case of fullerenes. ESR spectra were recorded on a Varian E-12A spectrometer. Temperature (295 K) was controlled using a "Unipan" device; g-factors were determined using the Varian standard with g-factor 2.0028.

2.1.1. Preparative Functionalization Procedures

A sample of purified SWNT (2.5 mg) was suspended (ultrasonic disruptor, 150 W, 35 kHz, 1 hour) in toluene (5 ml) saturated with argon, and a solid sample of the $[CpMo(CO)_3]_2$ dimer (1.8 mg) was added in an argon flow (1 : 57 mol C/mol dimer). The heterogeneous reaction mixture was stirred at 35 °C for 7 h under UV-irradiation. The reaction products were separated from the solution by vacuum filtration through a track membrane (pore size 0.2 μm; JINR, Dubna, Russia), washed with solvents and dried in air. Black solid films of the resulting materials of molybdenum-bonded SWNT ([Mo]-SWNT) were easily peeled off from the filter, dried for 8 h in vacuum at $T = 100$ °C and weighed.

2.2. Structural Characterization

The Raman spectra were acquired on a Jobin Yvon S-3000 spectrometer. The spectra were excited by irradiation of Ar+-ion laser (514.5 nm).

The X-ray photoelectron spectroscopy (XPS) data were obtained using a MK II VG Scientific spectrometer. Photoelectron processes were excited using an Al K_α source with photon energy of 1486.6 eV, and the vacuum in the analytical chamber was maintained at 5 10^{-10} Torr. Spectra were collected in the constant analyzer pass energy (fixed analyzer transmission, FAT) mode, with pass energy of 20 eV. The energy resolution determined as full width at half-maximum of the Au 4f7/2 photoelectron line is 1.1 eV. The C 1s XPS spectra were acquired with a 0.1 eV step size. The spectrometer energy scale was calibrated using Cu 2p3/2, Ag 3d5/2, and Au 4f photoelectron lines at 932.7, 368.3, and 84.0 eV, respectively.

TGA measurements were performed on a Perkin Elmer TGA Pyris 1 instrument with a heating rate of 25 °C min^{-1} up to 750 °C under air flow of 14l min^{-1}.

3. RESULTS AND DISCUSSION

3.1. ESR Spectroscopy

Now we wish to report the study of addition of the molybdenum-centered free radical to fullerenes and SWNT (Scheme 3).

$$[CpMo(CO)_3]_2 \xrightarrow{h\nu} 2[CpMo(CO)_3]^\bullet +$$

$$C_{60} \xrightarrow{Ar} \{CpMo(CO)_2(\eta^2 - C_{60})\}^\bullet$$

$$[CpMo(CO)_3]^\bullet + SWNT \xrightarrow{Ar}$$

$$\{SWNT - [CpMo(CO)_3]\}^\bullet \xrightarrow{Air} [Mo] - SWNT$$

Scheme 3

It is well-known that in the series of compounds $CpM(CO)_3$-$(OC)_3MCp$ the stability of the metal-metal bonds increases in the order Cr≪Mo < W. Whereas the chromium dimer undergoes the easy homolytical dissociation in toluene at room temperature, the same process for the molybdenum analogue requires UV irradiation in the ESR ampoule under argon during several hours. After that the radical-adducts formed persist for many days or even weeks. Satellites due to the magnetic isotope ^{95}Mo (nuclear spin $I = 5/2$, natural abundance 15.72%) have been nicely observable (Figs. 1, 2). The structure of this species can be assigned by analogy with the chromium compound as $\{CpMo(CO)_2(\eta^2\text{-}C_{60/70})\}^\bullet$, these radicals are characterized by $g = 2.029$ and $a(^{95}Mo) = 18.8$ G. The analogous tungsten dimer did not afford the fullerenyl radical-adduct under the same conditions. This is in correspondence with the greatest stability of the W–W bond in these dimers.

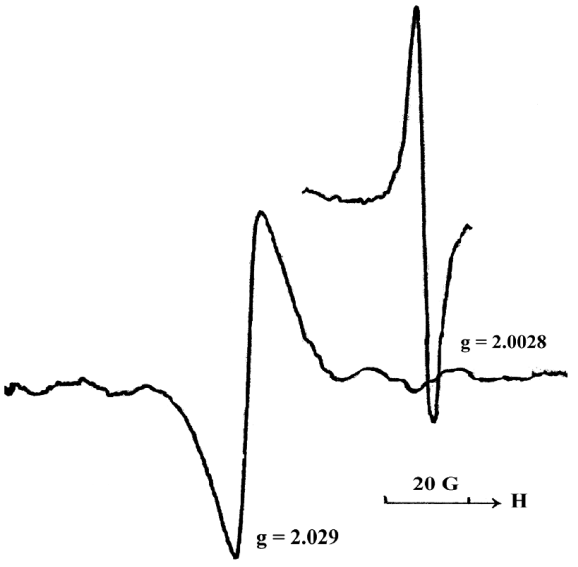

Fig. 1. ESR spectrum of the "Mo" radical-adducts of C_{60} (for C_{70} the same) in toluene at room temperature. Signal $g = 2.0028$ is from the standard.

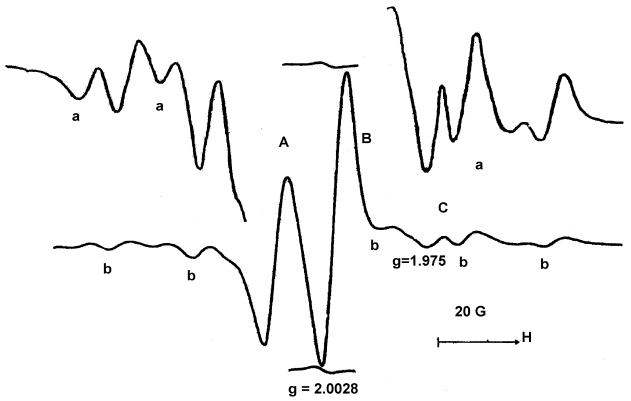

Fig. 2. ESR spectrum of the "Mo" radical-adducts of SWNT. For peaks A and B satellites are shown due to ^{95}Mo isotope. They were not observable for peak C of low intensity. Signal $g = 2.0028$ is from the standard.

ESR data for the "Cr" and "Mo" radical-adducts of both fullerenes and SWNT are summarized in Table I. Taking into account the similarity with the *fullerenylchromium* radical-adducts for which the η^2-structure was established by the detailed DFT calculations[8] we suggest the same structure for the *fullerenylmolybdenum* radical-adducts. The difference in the values of g-factor for "Mo" radical adducts of both fullerenes and SWNT (Table I) can originate from different nature of the radical interaction with fullerenes and carbon nanotubes. For example, similarly to chromium-centered free radical,[9] molybdenum-centered free radicals can also add to nanotubes via oxygen atoms located on either nanotube surface or edges.

3.2. Thermal Gravimetric Analysis

Figure 3 shows TGA loss weight curves in air for pristine SWNT (**1**) and [Mo]-SWNT (**2**) samples. TGA of **1** and **2** showed that the temperature of the beginning of weight loss significantly decreased in the molybdenum derivative : **1**-420 °C, **2**-300 °C. Lower temperature in 2 can be associated with the loss of a ligand (CO or/and cyclopentadienyl) from the molybdenum atom bound to the nanotube structure. Lower temperatures of combustion of **2** can be a result of a catalytic action of metallic molybdenum remaining on the nanotube surface after complex

Table I. Comparison of the ESR data for chromium and molybdenum radical-adducts of fullerenes and carbon nanotubes. $T = 295$ K.

	"Cr"		"Mo"	
	g-factor	a(^{53}Cr), G	g-factor	a(^{95}Mo), G
C_{60}	2.0134	13.25	2.029	18.8
C_{70}	2.0138	13.25	2.029	18.8
SWNT	1.9929	16.5	2.0008	33.0
	1.9938	15.0	2.0148	38.0
			1.9750	*
Ref.	8–(fullerenes) 9 – (nanotube)		This work	

*non-observable

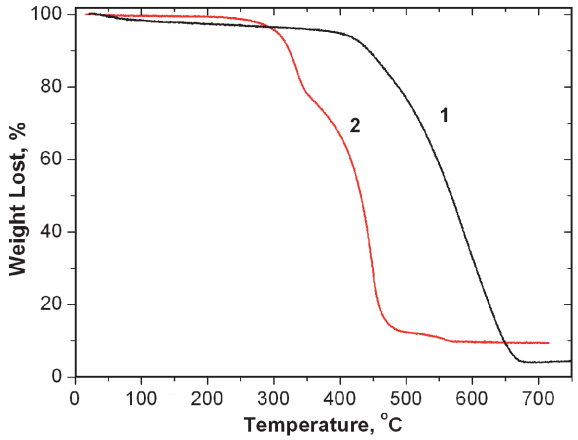

Fig. 3. TGA loss weight curves of pristine SWNT (**1**) and [Mo]-SWNT (**2**). 25 °C/min, air.

decomposition. The reverse phenomenon was observed in the course of nanotube purification from metal catalyst: lower metal content in a sample results in lowere temperature of combustion point.[14] The loss weight curve of **2** allows one to determine molybdenum content in functionalized tubes. An incombustible material remainder, which consists of iron and molybdenum oxides is 9.5% wt., the content of molybdenum being equal to 3.5% wt. That is the addition of molybdenum-centered free radicals to nanotubes two times less than chromium.[9]

3.3. Raman Spectroscopy

The Raman spectrum of SWNT (Fig. 4, **1**) displays two strong bands: so-called radial breathing (268 cm^{-1}) and tangential (1588 cm^{-1}) (G band) modes. A weaker band centered at ca. 1334 cm^{-1} (D band) is attributed to disorder or sp^3-hybridized carbons in the hexagonal framework of the nanotube walls. There are no remarkable differences between the Raman spectra of pristine SWNTs (**1**) and

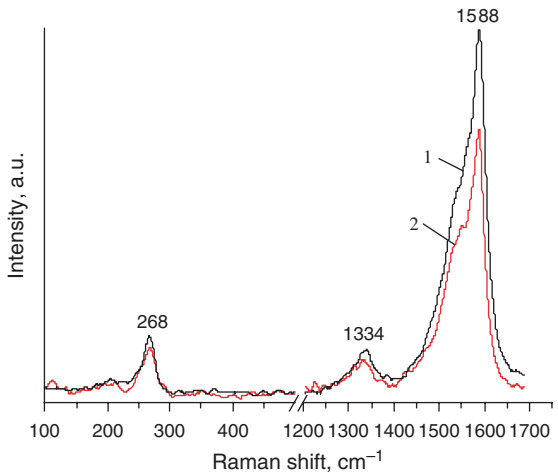

Fig. 4. Raman spectra ($\lambda_{ex} = 514.5$ nm) of pristine SWNT (**1**) and [Mo]-SWNT (**2**).

RESEARCH ARTICLE

Mo-functionalized SWNTs (**2**). The G band maximum at 1588 cm^{-1} remains unchanged for (**1**) and (**2**) samples. Its intensity (I) slightly decreased. Intensity ratio I_D/I_G for samples **1** ($I_D/I_G = 0.060$) and **2** ($I_D/I_G = 0.057$) remains constant (in frames of the experiment accuracy). These data are quite similar to our previous results on the interaction of the analogous chromium-centered free radicals with oxidized SWNT.[9] This is opposite to the earlier observed behavior of the covalent C-addition of aryl radicals to the sidewall of nanotubes, when the substantial increase of I_D/I_G ratio[12, 13] was observed. The absence of I_D/I_G ratio variation for the sample 2 may be explained by a low percentage of functionalization of the pristine SWNTs by molybdenum-centered free radicals. For these radicals the percentage is 3.5%wt. This is much less than in case of addition of chromium-centered radicals (7%wt.)[12] and C-centered radicals (21%wt.).[13] However, it was reported[14] that I_D/I_G ratio decreased upon the formation of oxygen-metal-functionalized adducts of SWNT. The increase in *D* band intensity in functionalized tubes is usually associated with the formation of a covalent bond between a functional group and a sidewall of nanotubes, which results in a conversion of a significant amount of sp^2-hybridized carbon into sp^3-hybridized carbon.[15] The absence of this effect upon the addition of molybdenum-centered free radicals to nanotubes indicates that these radicals interact with SWNTs without changing the type of hybridization of the surface carbon atoms of nanotubes. Probably, the addition of molybdenum-centered free radicals to the nanotubes without change of hybridization type of the surface carbon atoms occurs as a connection via oxygen atoms. Oxygen concentration in sidewalls and ends of nanotubes is quite high (4 at.%, Table II). The Raman data obtained are not contradictory with such mechanism, but for the final conclusion the data of other techniques are needed.

3.4. X-Ray Photoelectron Spectroscopy

XPS of [Mo]-SWNT showed the presence of carbon, molybdenum and oxygen in the survey spectrum (Fig. 5).

A comparison of the C1s core level of [Mo]-SWNT (**2**) sample with the spectrum of pristine SWNT (**1**) is shown in Figure 6. The C1s core level of the functionalized sample is located at a binding energy that is by 0.2 eV lower than that of pristine SWNT. The C1s core level shift is explained by the transfer of negative charge from the SWNTs to molybdenum. The similar effect is observed with acid-treated SWNTs, where a positive charge on the SWNTs leads to reduction of the C1s binding energy.[16]

Table II. Atomic concentrations calculated from XPS experimental data for pristine purified SWNT and [Mo]-SWNT samples.

	Atomic concentrations of elements, at.%				
Sample	C	O	Mo	Cl	Fe
Pristine SWNT	95.0	4.0	—	0.6	0.4
[Mo]-SWNT	91.5	7.5	0.6	—	0.4

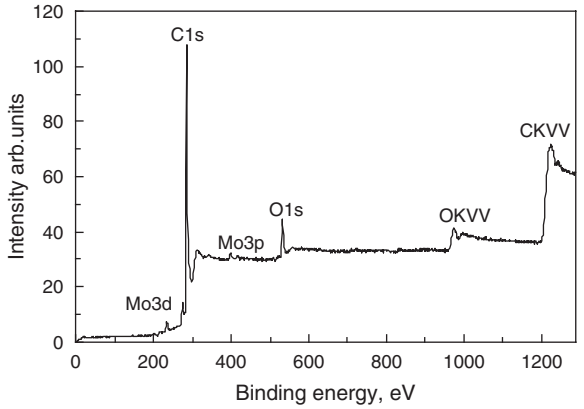

Fig. 5. XPS analysis of SWNT functionalized using molybdenum-centered free radicals.

On the basis of these XPS results, the C1s, O1s, and Mo3d peak areas were determined. The atomic concentration values given in Table II were based on the peak areas and calculated using sensitivity factors 0.25, 0.66, and 2.75 for carbon, oxygen, and molybdenum, respectively.[17] From these data relative content of the elements in the sample [Mo]-SWNT can be calculated to get C : O : Mo = 153 : 12.5 : 1. Thus, in the radical addition reaction one Mo atom is per 7 O atoms of nanotube considering that pristine SWNT contains 4 at.% of oxygen (Table II). TGA of Mo-SWNT materials (air, 25 °C/min to 750 °C) showed the comparable weight loss that is calculated to be ca. 3.5%wt. Mo (0.6 at.%).

In the XP spectrum of [Mo]-SWNT and the deconvolution of the Mo 3d spectrum (Fig. 7) indicates that the spectrum is the results of a superposition of two different Mo 3d spectra. The first component has $3d_{5/2}$ binding energy 230.5 eV amounting to about 19% and second one—$3d_{5/2}$ binding energy 232.7 eV amounting to about 81%. Binding energy of Mo $3d_{5/2}$ in $[CpMo(CO)_3]_2$ dimer measured in this study exhibited values 228.3 eV.

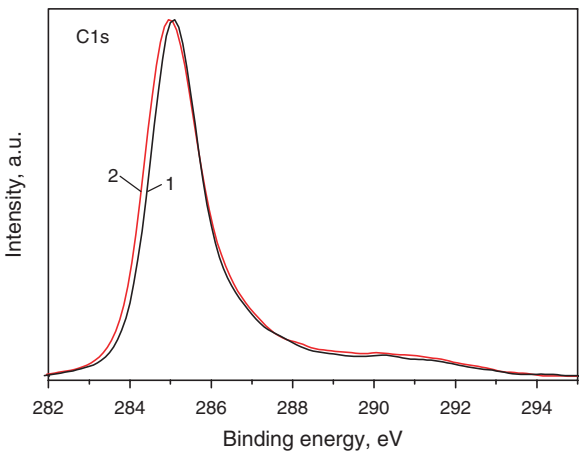

Fig. 6. C1s core level of pristine SWNT (**1**) and [Mo]-SWNT (**2**).

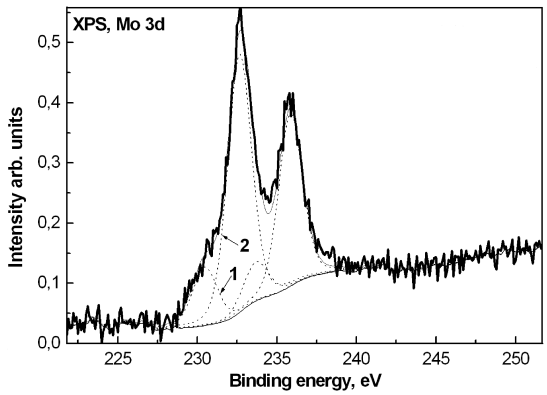

Fig. 7. Mo 3d spectrum of [Mo]-SWNT and the deconvolution XP spectrum which were fitted to a 3.2 eV separation between the $3d_{5/2}:3d_{3/2}$ lines of doublet with resulting intensity ratios of approximately 3 : 2. Components of XP spectra: (1) - $3d_{5/2}$ binding energy 230.5 eV; (2) - 232.7 eV.

XPS data show that addition of $[CpMo(CO)_3]^\bullet$ to SWNT results in the occurrence on the nanotube surface molybdenum compounds with various oxidation states. Binding energy $Mo3d_{5/2}$ of these compounds are higher than bonding energy $Mo3d_{5/2}$ in the starting dimer $[CpMo(CO)_3]_2$ by 2.2 eV and 4.4 eV. Formal oxidation state of Mo in [Mo]-SWNT is (+2) and (+4) as follows from the Mo 3d XPS data measured in this work and taken from the literature.[18] High oxidation state of molybdenum can be explained by the air oxidation after the addition of molybdenum-centered free radicals to the nanotubes surface.

4. CONCLUSION

Metal-centered free radicals $[CpMo(CO)_3]^\bullet$ generated photochemically from the corresponding dimer $[CpMo(CO)_3]_2$ react with fullerenes C_{60}, C_{70} or single-walled carbon nanotubes in toluene to give the radical-adducts to which the structures of η^2-fullerenyl and [Mo]-SWNT species have been assigned on the basis of ESR, TGA, Raman, and XPS studies and similarity to the chromium analogues previously investigated. Such functionalized carbon nanotubes involving the addition of molybdenum metal complex can be useful for the development of new supported catalysts with interesting catalytic properties.

Acknowledgments: Federal Agency for Science of the Ministry of Education (contract 02.434.11.2023) and Russian Foundation for Basic Research (grants 05-03-33132, 04-02-17618) are thanked for the financial support.

References and Notes

1. P. J. Krusic, E. Wasserman, B. A. Parkinson, P. N. Keizer, J. R. Morton, and K. F. Preston, *Science* 254, 1183 (**1991**).
2. B. L. Tumanskii, V. V. Bashilov, S. P. Solodovnikov, and V. I. Sokolov, *Russ. Chem. Bull. [Engl.]* 41, 1140 (**1992**).
3. B. L. Tumanskii and O. G. Kalina, Radical Reactions of Fullerenes and Their Derivatives, Kluwer Academic Publ., Dordrecht (**2001**).
4. B. L. Tumanskii, V. V. Bashilov, S. P. Solodovnikov, and V. I. Sokolov, *Russ. Chem. Bull. [Engl.]* 41, 1521 (**1992**).
5. B. L. Tumanskii, V. V. Bashilov, S. P. Solodovnikov, and V. I. Sokolov, *Russ. Chem. Bull. [Engl.]* 44, 1771 (**1995**).
6. R. G. Gasanov, B. L. Tumanskii, M. V. Tsikalova, I. A. Nuretdinov, V. P. Gubskaya, V. V. Zverev, and G. M. Fazleeva, *Russ. Chem. Bull. [Engl.]* 51, 2491 (**2002**).
7. V. V. Bashilov, B. L. Tumanskii, P. V. Petrovskii, and V. I. Sokolov, *Russ. Chem. Bull. [Engl.]* 43, 1069 (**1994**).
8. V. I. Sokolov, R. G. Gasanov, L. Y. Goh, Z. Weng, A. L. Chistyakov, and I. V. Stankevich, *J. Organomet. Chem.* 690, 2333 (**2005**).
9. A. S. Lobach, R. G. Gasanov, E. D. Obraztsova, A. N. Shchegolikhin, and V. I. Sokolov, *Fullerenes, Nanotubes, and Carbon Nanostructures* 13, 287 (**2005**).
10. I. W. Chiang, B. E. Brinson, R. E. Smalley, J. L. Margrave, and R. H. Hauge, *J. Phys. Chem. B* 105, 1157 (**2001**).
11. A. S. Lobach, N. G. Spitsina, S. V. Terekhov, and E. D. Obraztsova, *Phys. Solid. State* 44, 475 (**2002**).
12. A. S. Lobach, V. V. Solomentsev, E. D. Obraztsova, A. N. Shchegolikhin, and V. I. Sokolov, Electronic properties of synthetic nanostructures, edited by H. Kuzmany, S. Roth, M. Mehring, and, J. Fink, AIP Conference Proceedings, New York (**2004**), Vol. 723, p. 209.
13. B. K. Price, J. L. Hudson, and J. M. Tour, *J. Am. Chem. Soc.* 127, 14867 (**2005**).
14. T. Hemraj-Benny, S. Banerjee, and S. S. Wong, *Chem. Mater.* 16, 1855 (**2004**).
15. M. Holzinger, J. Abraham, P. Whelan, R. Graupner, L. Ley, F. Hennrich, M. Kappes, and A. Hirsch, *J. Am. Chem. Soc.* 125, 8566 (**2003**).
16. R. Graupner, J. Abraham, A. Vencelova, T. Seyller, F. Hennrich, M. M. Kappes, A. Hirsch, and L. Ley, *Phys. Chem. Chem. Phys.* 5, 5472 (**2003**).
17. D. Briggs and M. P. Seah (Eds.), Practical Surface Analysis by Auger and X-ray Photoelectron Spectroscopy, John Wiley and Sons Ltd., Chichester (**1983**).
18. S. J. N. Burgmayer, H. L. Kaufmann, G. Fortunato, P. Hug, and B. Fischer, *Inorg. Chem.* 38, 2613 (**1999**).

Received: 29 January 2006. Accepted: 11 July 2006.

RESEARCH ARTICLE